

# Thermal Analysis in Thermoset Characterization

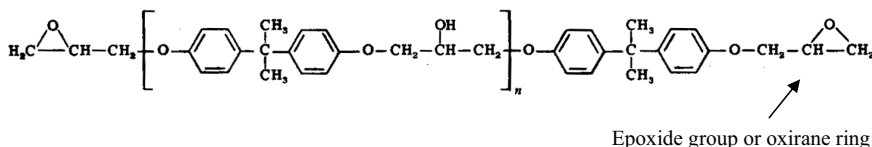
R. Bruce Prime  
IBM (Retired) / Consultant  
rbprime@attglobal.net

Thermosetting polymers are unique. Unlike thermoplastic polymers, chemical reactions are involved in their use. As a result of these reactions the materials cross-link and become “set”, i.e. they can no longer flow or dissolve. Cure most often is thermally activated, hence the term “thermoset”, but cross-linking materials whose cure is light activated are also considered to be thermosets. Some thermosetting adhesives cross-link by a dual cure mechanism, that is by either heat or light activation. Prime [1] is a general reference for this article.

In this paper the distinguishing characteristics of thermosetting materials will be described, followed by a detailed description of thermal analysis of the cure process, some brief comments on properties of cured thermosets and concluding with a discussion of kinetics including a recent case study. Note that Dynamic Mechanical Analysis of Thermosets is treated in a separate paper.

Uncured thermosets are mixtures of small reactive molecules, often monomers. They may contain additives such as particles or fibers to enhance physical properties or reduce cost. Adhesives are probably the most common application of thermosets but they are also found in aerospace, electronic, medical and dental, and recreational materials.

The most common thermoset is epoxy, and the most common epoxy resin is the diglycidyl ether of bisphenol-A:



The number of repeat units  $n$  is usually 0-6, 0 being the monomer. Epoxy resins can cross-link with themselves, referred to as homopolymerization, an example of which is anionic polymerization promoted by imidizoles. But it is more common to cross-link epoxies with a co-reactant such as a diamine. For cross-linking to occur at least one of the reactants must be trifunctional or higher. Epoxy resins are typically difunctional, reacting through the oxirane group, although in some cases reaction can occur through the -OH group. Diamines are four-functional where each amine hydrogen can react. The heat of reaction  $\Delta H_{rxn}$  for epoxy-amine is  $\sim 25\frac{1}{2}$  kcal/mole ( $\sim 106$  kJ/mol) and the activation energy for cure can vary from 10 to 25 kcal/mole (40-100 kJ/mol) depending on the particular epoxy and curing agent.

Two distinct phenomena are characteristic of thermoset curing, gelation and vitrification. Gelation is the transformation from a liquid to an elastic gel or rubber and it will always occur in a thermoset. Gelation is abrupt and irreversible and the gel point can be defined as the instant at which the molecular weight becomes infinite [2]. A thermoset is no longer processable above the gel point and therefore gelation defines the

upper limit of the work life. For a “Five Minute Epoxy” the five minutes refers to the gel point at room temperature (RT). For example, after the two parts are mixed the user must form an adhesive joint within five minutes before the material becomes rubbery. However, completion of cure requires a much longer time at RT but may be shortened by increasing the temperature. The degree of conversion at the gel point  $\alpha_{\text{gel}}$  is constant for a given thermoset, independent of cure temperature, i.e. gelation is iso-conversional. Therefore the time to gel versus temperature can be used to measure the activation energy for cure. Gelation does not affect the rate of cure and therefore is not detected directly by DSC but only indirectly if  $\alpha_{\text{gel}}$  is known. Gelation is detected directly by rheology and DMA and because it is a specific point along the reaction path it is determined by the chemical reaction and therefore independent of frequency. Vitrification is a completely distinct phenomenon that may or may not occur during cure depending on the cure temperature relative to the  $T_g$  for full cure. Vitrification is the glass transition due to reaction and occurs when the increasing  $T_g$  becomes equal to the cure temperature, i.e. when  $T_g = T_{\text{cure}}$ . Vitrification can occur anywhere during the reaction to form either an ungelled glass or a gelled glass. It can be avoided by curing at or above  $T_{g\infty}$ , the glass transition temperature for the fully cured network. Unlike gelation, vitrification is reversible by heating. Also unlike gelation it causes a shift from chemical control to diffusion control and a dramatic slowing of the reaction. Vitrification is detected by TMDSC and DMA as a frequency-dependent transition.

Thermoanalytical techniques include differential scanning calorimetry (DSC), rheology, dynamic mechanical analysis (DMA), thermal mechanical analysis (TMA) and thermogravimetric analysis (TGA). DSC measures heat flow into a material (endothermic) or out of a material (exothermic). Thermoset cure is exothermic. DSC applications include measurement of  $T_g$ , conversion  $\alpha$  from the area under the exotherm, the reaction rate  $d\alpha/dt$  and the heat capacity  $C_p$ . Gelation cannot be detected by DSC but vitrification can be measured by modulated-temperature DSC (MTDSC). Rheology measures the complex viscosity in steady or oscillatory shear. In oscillatory shear the advance of cure can be monitored through the gel point and both gelation and the onset of vitrification can be detected. DMA measures the complex modulus and compliance in several oscillatory modes. Gelation and vitrification can be detected, and the cure reaction can be monitored beyond the gel point in the absence of vitrification.  $T_g$ , secondary transitions below  $T_g$ , creep and stress relaxation can also be measured. TMA measures linear dimensional changes with time or temperature, sometimes under high loading. Measurements include linear coefficient of thermal expansion (CTE),  $T_g$ , creep and relaxation of stresses. TGA measures mass flow, primarily in terms of weight loss. Measurements include filler content for inert fillers; weight loss due to cure, e.g. loss of water for condensation reactions; outgassing; moisture sorption and desorption; and thermal and thermo-oxidative stability.

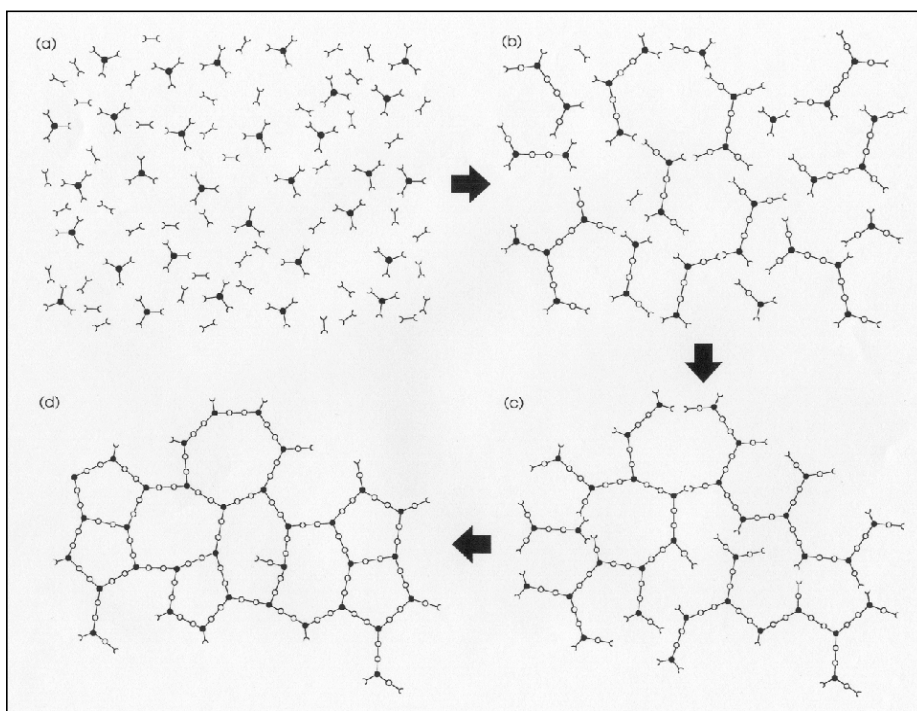


*Figure 1. Schematic, two-dimensional representation of thermoset cure. For simplicity difunctional and trifunctional co-reactants are considered. Cure starts with A-stage monomers (a); proceeds via simultaneous linear growth and branching to a B-stage material below the gel point (b); continues with formation of a gelled but incompletely cross-linked network (c); and ends with the fully cured, C-stage thermoset (d). From Ref. 1.*

Cure is illustrated schematically in Fig. 1 for a material with co-reactive monomers such as an epoxy-diamine system. For simplicity the reaction of a difunctional monomer with a trifunctional monomer is considered. Reaction in the early stages of cure {(a) to (b) in Fig. 1} produces larger and branched molecules and reduces the total number of molecules. Macroscopically the thermoset can be characterized by an increase in its viscosity  $\eta$  (see Fig. 2 below). As the reaction proceeds {(b) to (c) in Fig. 1}, the increase in molecular weight accelerates and all the chains become linked together at the gel point into a network of infinite molecular weight. The gel point coincides with the first appearance of an equilibrium (or time-independent) modulus as shown in Fig. 2. Reaction continues beyond the gel point {(c) to (d) in Fig. 1} to complete the network formation. Macroscopically physical properties such as modulus build to levels characteristic of a fully developed network.

Fig. 3 shows DSC after isothermal cure at 160°C at various stages of cure for a typical epoxy-amine from uncured to fully cured. Note the residual exotherm decreasing and the  $T_g$  increasing in step with cure time. DSC at 10°C/min. From Ref. 4.

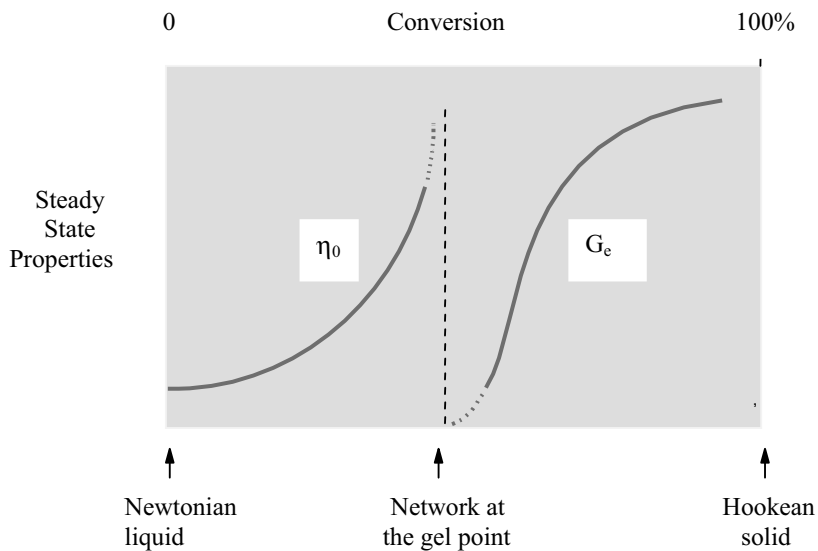


Figure 2. Macroscopic development of rheological and mechanical properties during network formation, illustrating the approach to infinite viscosity and the first appearance of an equilibrium modulus at the gel point. From Ref. 3.

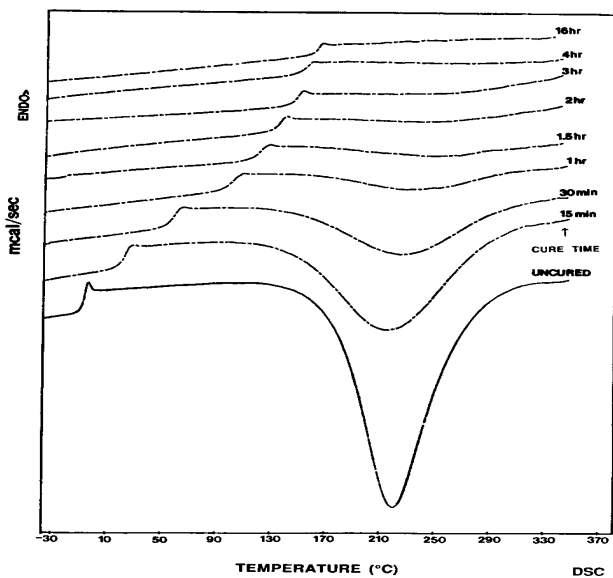


Figure 3.

Fig. 4 shows conversion-time curves for the same epoxy for cure temperatures from 100° to 180°C [4]. Note that the curves are parallel during the first part of cure.

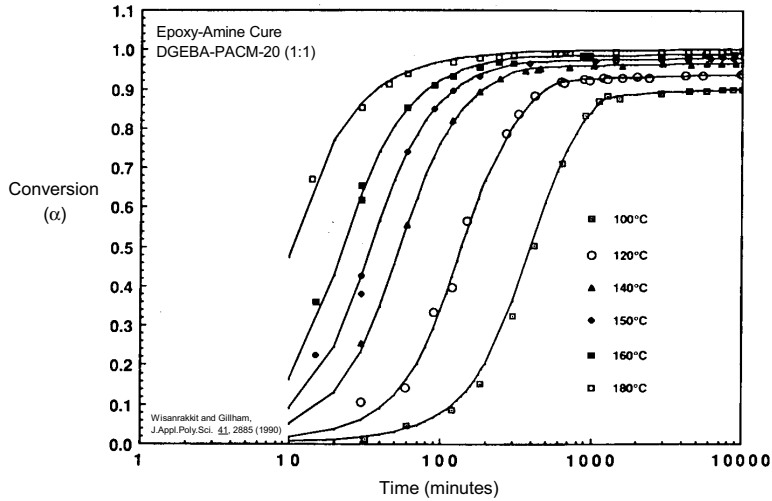
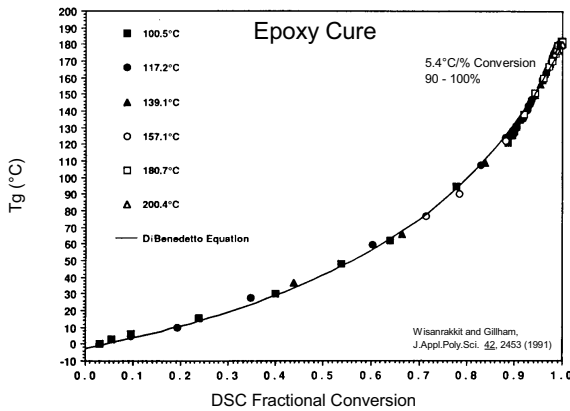


Figure 4.



$$\ln(T_g) = \frac{(1 - \alpha) \ln(T_{g0}) + \frac{\Delta C_{p\infty}}{\Delta C_{p0}} \alpha \ln(T_{g\infty})}{(1 - \alpha) + \frac{\Delta C_{p\infty}}{\Delta C_{p0}} \alpha}$$

Venditti and Gilham, J.Appl.Poly.Sci. 65, 3, (1997)

Figure 5.

Fig. 5 shows the  $T_g$  - conversion relationship for the same epoxy fitted to the DiBenedetto equation [5]. Note that as cure progresses  $T_g$  becomes an increasingly more sensitive measure of cure relative to the residual exotherm. From Ref. 4. Also shown is the Venditti-Gillham equation [6] relating  $T_g$  and conversion.

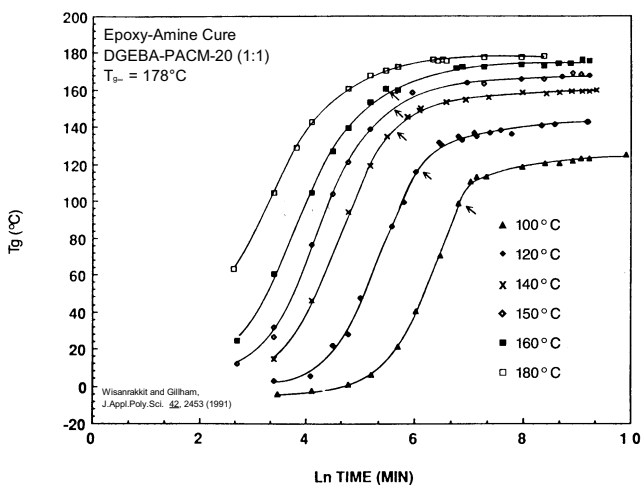


Figure 6.

Fig. 6 shows the  $T_g$  - time curves for the same epoxy system [4]. Note the similarity to the conversion - time curves. The arrows indicate vitrification.

Dynamic mechanical analysis (DMA) measures the complex modulus and compliance as a function of temperature, time and frequency where, for example,

- storage modulus ( $E'$ ,  $G'$ ) which is a measure of stress stored in the sample as mechanical energy
- loss modulus ( $E''$ ,  $G''$ ) which is a measure of the stress dissipated as heat
- $\tan \delta$  ( $E''/E' = G''/G'$ ) which is the phase lag between stress and strain

Properties measured include storage and loss modulus, storage and loss compliance,  $\tan \delta$ ,  $T_g$ , secondary transitions below  $T_g$ , gelation and vitrification and reaction beyond the gel point. DMA of thermosets is covered in a subsequent paper. Gelation is the first appearance of a cross-linked network. It is the irreversible transformation of a liquid to a gel or rubber and it is accompanied by a small increase in the storage modulus. A distinction may be drawn between molecular or chemical gelation (the phenomenon) and macroscopic gelation (its consequence). Chemical gelation as defined by Flory is the approach to infinite molecular weight. It is an iso-conversional point ( $\alpha_{gel}$ ) that is observable as the first detection of insoluble, cross-linked gel in a reacting mixture (sol). Chemical gelation is also defined as the point where  $\tan \delta$  becomes frequency independent [2]. Macroscopic gelation may be observed as the approach to infinite viscosity, the first evidence of an equilibrium modulus, the  $G' = G''$  crossover in a rheology measurement, or as a loss peak in fiber and mesh supported systems.

Vitrification is distinct from gelation. It is glass formation due to  $T_g$  increasing from below  $T_{cure}$  to above  $T_{cure}$  as a result of reaction. It only occurs when  $T_{cure} < T_{g\infty}$  and begins when  $T_g = T_{cure}$  (the definition of vitrification). Vitrification is reversible by heating: liquid or gel  $\Leftrightarrow$  glass. It causes a dramatic slowing of rate of cure as a result

of a shift in the reaction from chemical control to diffusion control. Vitrification is mechanically observable as a large increase in modulus and frequency dependent loss peak (note that vitrification occurs at shorter times with increasing frequency, i.e. it is not iso-conversional). This phenomenon is illustrated in the companion paper on Dynamic Mechanical Analysis of Thermosetting Materials. It is also observable by MTDSC as a step decrease in heat capacity, as demonstrated in Fig. 7 below during the slow heating of an acid anhydride cured epoxy [7]. 1 = heat, 2 = cool). Note that the onset of vitrification at  $\sim 100^\circ\text{C}$  results in a diminished rate of cure under diffusion control until cure is complete at  $\sim 140^\circ\text{C}$ .

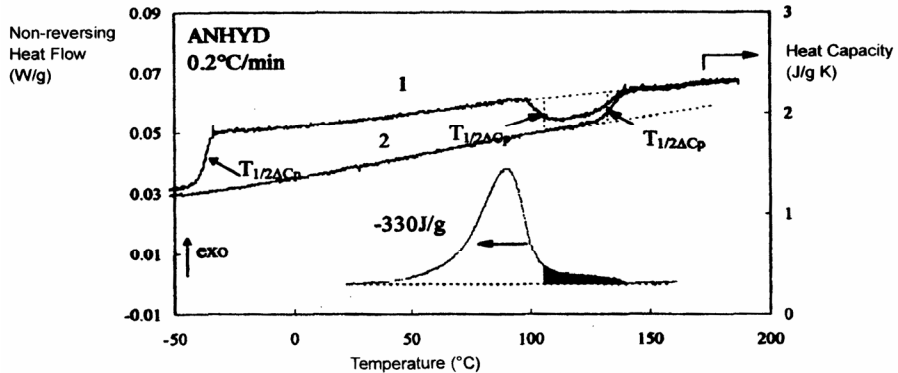


Figure 7.

Fig. 8 shows the non-isothermal cure of the same epoxy-anhydride at three heating rates as well as for the fully cured material. Only at the fastest heating rate does cure proceed to completion without vitrification. From Ref. 7, courtesy M. Reading, 1 = 0.2, 2 = 0.4 and 3 = 0.7°C/min.

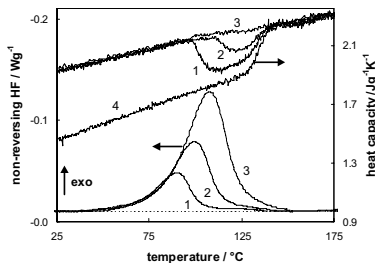


Figure 8.

Thermomechanical analysis (TMA) measures linear dimensional changes in a material with temperature, time or applied load.  $T_g$  and the linear coefficient of thermal expansion (CTE) may be measured as well as irreversible expansion or contraction due to relaxation of stresses on heating through the glass transition. Creep or time-dependent strain under load may also be determined. Fig. 9 shows classical TMA in the expansion mode on heating [1]. CTE ( $\alpha$ ) may be measured from the slope of the TMA curve below and above  $T_g$  or it may be read directly from the derivative DTMA curve. CTE in the rubbery state ( $\alpha_2$ ) is typically  $\sim 3x$  that in the glassy state ( $\alpha_1$ ). Note the similarity of the DTMA curve to heat capacity through the  $T_g$  interval. Also note that obtaining a “textbook” curve such as this usually requires a preheat to just above  $T_g$  to relieve any residual stress.

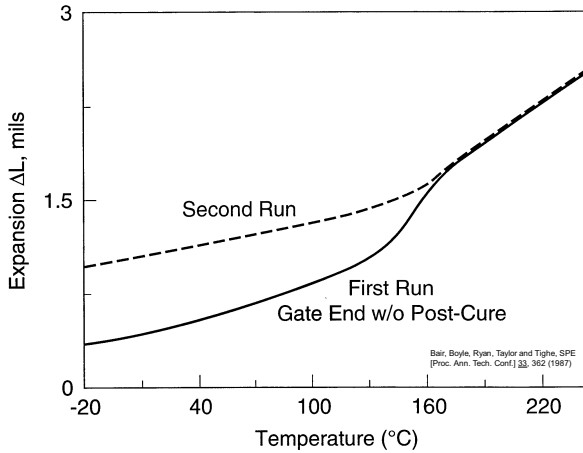


Figure 9.

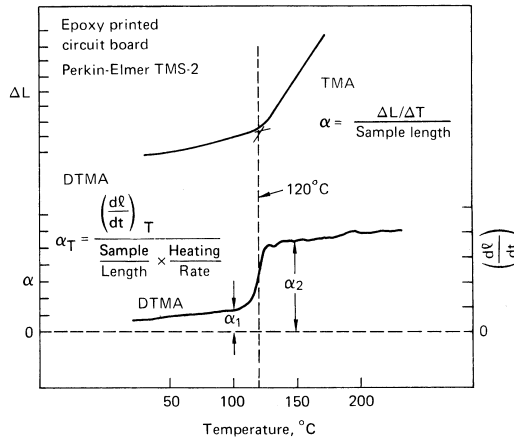


Figure 10.



Fig. 10 shows the thermal expansion and stress relief of a transfer molded integrated circuit (IC) device [8]. Note that the IC device is small enough to fit into the TMA sample chamber. On the first run notice the accelerating expansion as the temperature approaches  $T_g$  ( $\sim 160^\circ\text{C}$ ). This is due to the relief of molded in and other residual stresses. From the second run CTE values may be calculated as well as irreversible dimensional change due to the relaxation of stresses.

Thermogravimetric analysis (TGA) measures mass flow,  $\Delta W$ , out of a material (volatility, degradation) as a function of temperature, time and atmosphere. Properties measured include evaporation of volatile components due to outgassing and cure, filler content for inert fillers (carbon/graphite contents can be estimated from nitrogen-followed-by-air pyrolyses), thermal and thermo-oxidative stability, and degradative weight loss.

Fig. 11 shows two-step isothermal TGAs in dry  $\text{N}_2$  for a UV cured acrylic coating cured at three doses designated “High”, “Typical”, and “Low” [9]. Note how weight loss at  $150^\circ\text{C}$  tracks cure dose suggesting that uncured acrylic monomer contributes to outgassing.

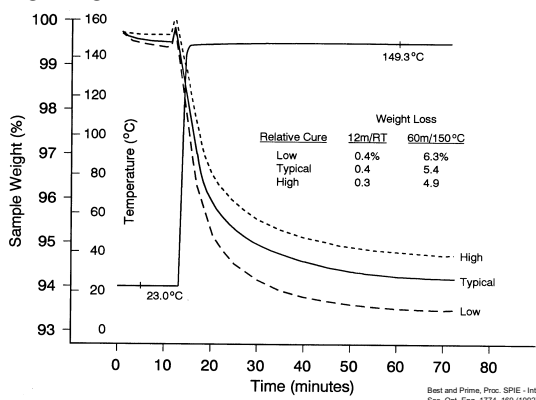


Figure 11.

Fig. 12 compares both room temperature and elevated temperature volatility of three acrylic coatings cured with the same “Typical” dose [9]. Coating 1 is from the previous slide. Note that Coating 2 exhibits the greatest RT weight loss but the lowest weight loss at  $150^\circ\text{C}$ . The authors attributed the high RT weight loss to greater water sorption capacity for this coating. Similar coatings are used for optical storage compact discs. The same authors showed that uncured acrylate monomers in these coatings will hydrolyze to form acrylic acid which is corrosive to the recording materials. Similar outgassing is also harmful inside hard disk drives.

Fig. 13 begins the discussion of kinetics, especially cure kinetics but degradation and aging kinetics may be treated in the same manner [1]. The methodology described here may be characterized as model-free kinetics where the activation energy  $E$  is constant. The assumption of a single or overall activation energy applies when the only effect of temperature is to speed up or slow down the reaction. This assumption applies well to most thermoset systems, a notable exception being those that exhibit multiple DSC exotherms. As illustrated below, when  $E$  is constant conversion-time curves (or  $T_g$ -time curves through the  $T_g$ -conversion relationship) will be parallel on a  $\ln(\text{time})$

plot, allowing construction of master cure or aging curves via time-temperature superposition.

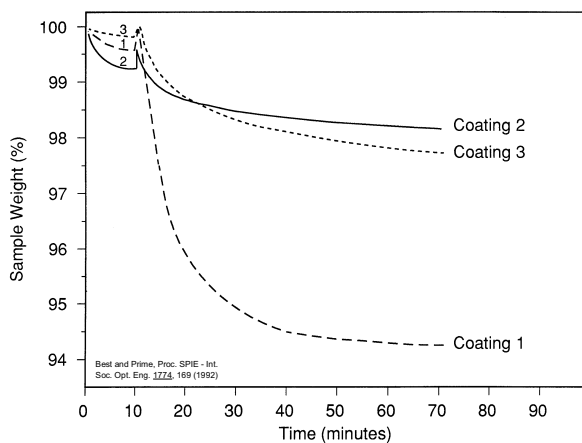


Figure 12.

The shift factor  $a_T$  is described by the Arrhenius equation where  $t$  is the time to constant conversion or constant  $T_g$ . Master curves are useful for succinctly summarizing all of the kinetic data and for predicting behavior at times and temperatures that may be of interest. It is recommended that behavior be predicted within the range of temperatures measured but estimates outside these limits can often be useful.

Fig. 14. shows the same  $T_g - \ln(\text{time})$  curves for epoxy-amine cure shown earlier in Fig. 6 [4]. Note the parallel nature of the curves prior to vitrification which is demarcated with arrows.

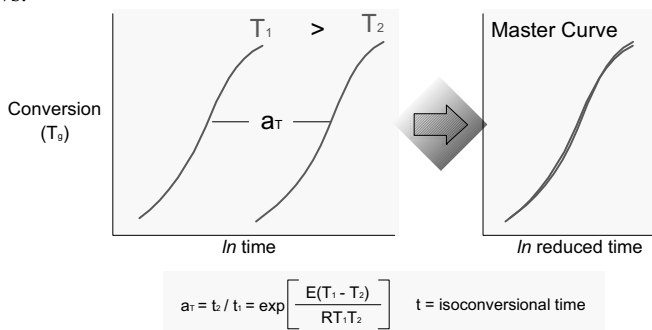


Figure 13.

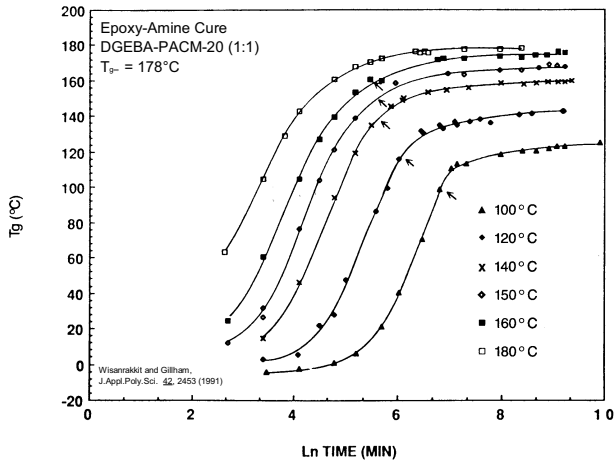


Figure 14.

Below in Fig. 15 is the master curve from shifting the above data along the  $\ln(\text{time})$  axis using the measured activation energy [4]. This curve clearly shows the reaction under chemical control (solid line) as well as the shift to diffusion control following vitrification.

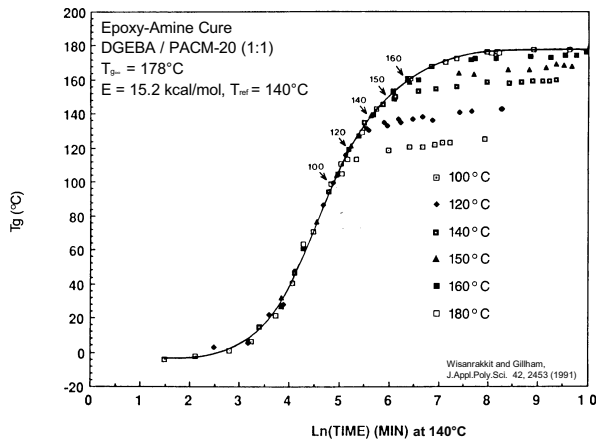


Figure 15.

Fig. 16 shows DSC conversion – time data for a low modulus adhesive with  $T_g$  close to room temperature [10]. One application of this adhesive is to produce bonded joints with low residual stress.

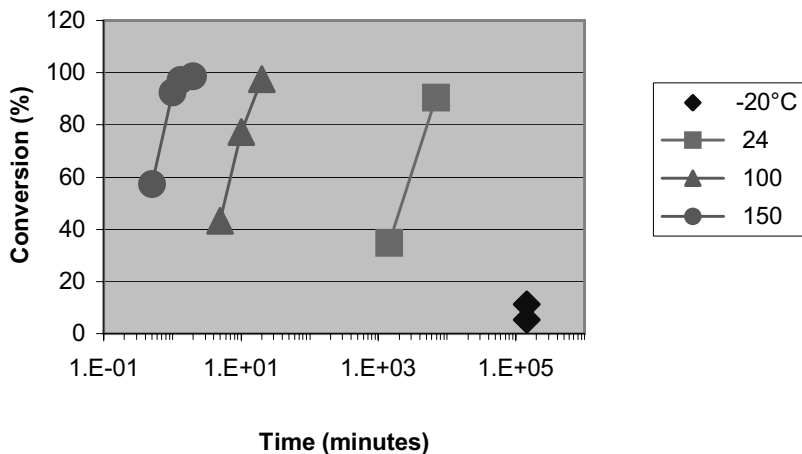


Figure 16.

The data above were shifted along the  $\ln(\text{time})$  axis by varying the activation energy  $E$  in an Excel spreadsheet to create master curve shown in Fig. 17 [10]. In this case  $E$  was determined from the best fit of the data. The reference temperature was chosen to be the maximum oven temperature allowed by the process, 120°C. Cure can be seen to be complete in 10 minutes at 120°C.

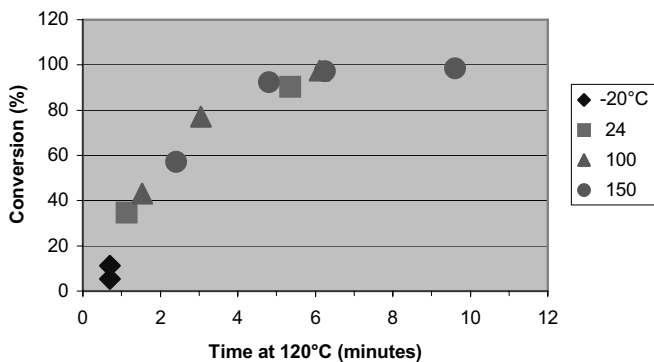


Figure 17.

Fig. 18 shows the same master curve at a reference temperature of 180°C [10]. The question prompting this curve was “What temperature will be required for cure to be complete in 30 seconds?”.

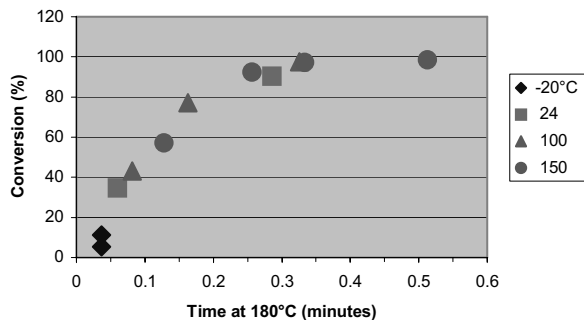


Figure 18.

This paper will conclude with presentation of an actual case study. The full paper [11] will be presented at the NATAS Conference in Albuquerque, NM, September 2003. The subject is a fast curing, two-component polyurethane. Parts are made by mixing the components in-line and rapidly processing and curing. The objective of this study was to determine the kinetic equation for cure for input into process modeling software. Below in Fig. 19 is a typical time-temperature profile for cure of the parts.

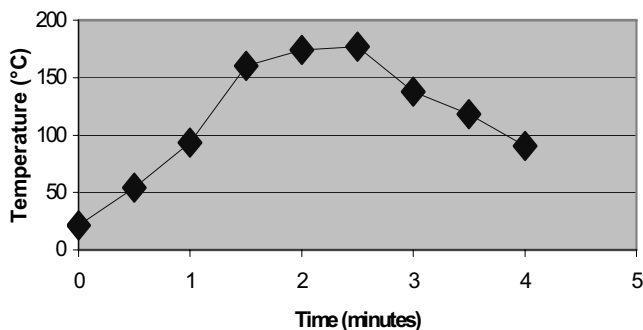


Figure 19.

Fig. 20 shows the time-temperature profile together with the desired output, the development of conversion along the profile. Following is the path taken to arrive at this endpoint.

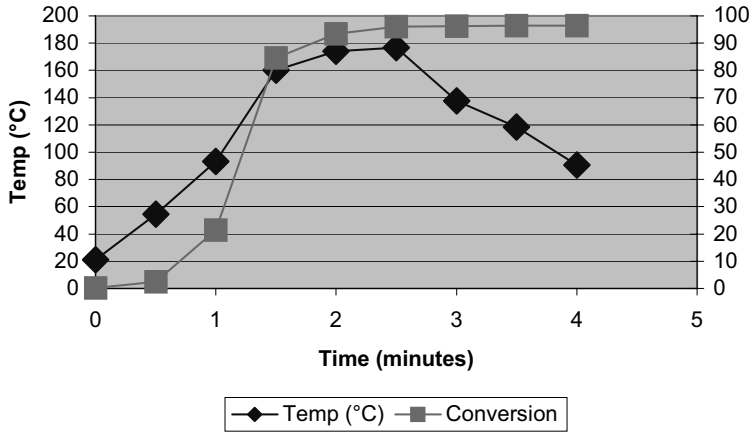


Figure 20.

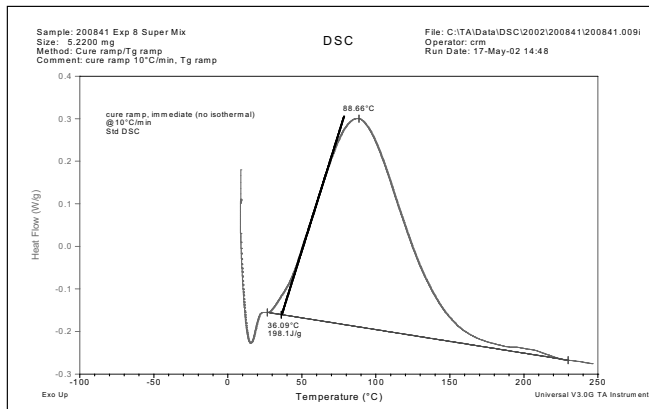


Figure 21.

Fig. 21 shows the DSC at 10°C/min of the uncured two-component polyurethane. Note the onset of the cure exotherm near 30°C which necessitated rapid mixing and sample preparation and chilling of the DSC prior to measurement. While a small secondary exotherm was noted near 200°C it was decided to ignore this because it was small and possibly due to errors in mixing.

We can now state the objective, which was to experimentally evaluate the parameters of the kinetic equation  $\{E, f(\alpha) \text{ and } A\}$  where

$$d\alpha/dt = k f(\alpha), k = A \exp[-E/RT] \quad (1)$$

and the step-by-step strategy to get there:

1. determine E from multiple heating rate measurements
2. develop the conversion-time master curve from isothermal measurements
3. determine  $f(\alpha)$  and k from the shape of the master cure curve
4. determine A from the Eq. 1 as the only remaining unknown

The results of Step 1 are shown in the Ozawa plot of peak temperature versus heating rate in Fig. 22. Corrections applied to the raw data yielded an activation energy E of 14.4 kcal/mole. See General Reference for procedural details.

$$E \sim -R / 1.052 \times \text{Slope} = 14.1 \text{ kcal/mole}$$

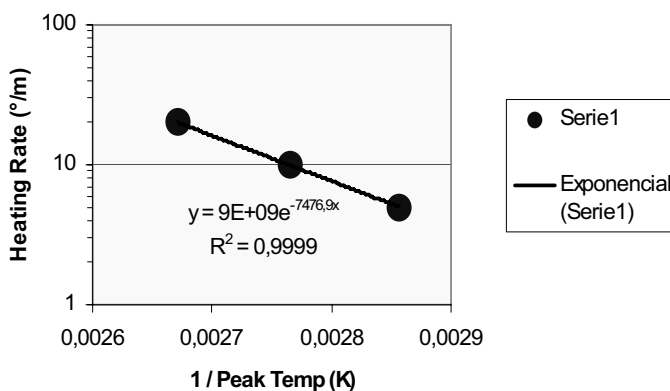


Figure 22.

In Step 2 conversion – time data were obtained by curing samples for various times in the DSC followed by 10°C/min scans to measure the residual exotherm. Conversion was measured from the residual exotherms and the heat of reaction  $\Delta H_{rxn}$  measured as the average of scans at 5, 10 and 20°C/min on the uncured thermoset. Scans on partially cured thermoset also gave  $T_g$  from which the  $T_g$  – conversion relationship was constructed. Shown in Fig. 23 is the unshifted conversion – time data.

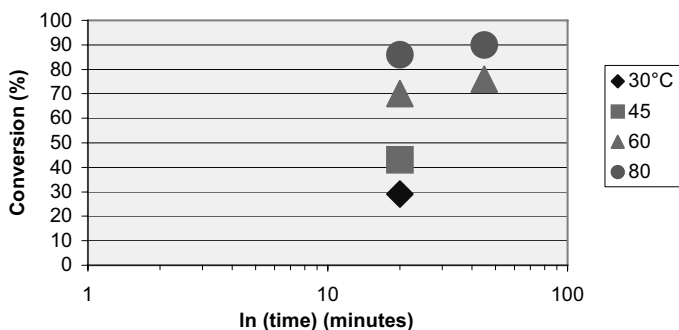


Figure 23.

These data were shifted to a reference temperature of 80°C by means of Eq. 2, using the activation energy measured in Step 1. Note that 80°C  $\equiv$  353K.

$$T_{80^{\circ}\text{C}} = t_{\text{T}} [E(T-80) / R(T+273)(353)] \quad (2)$$

The resulting master curve is shown in Fig. 24.

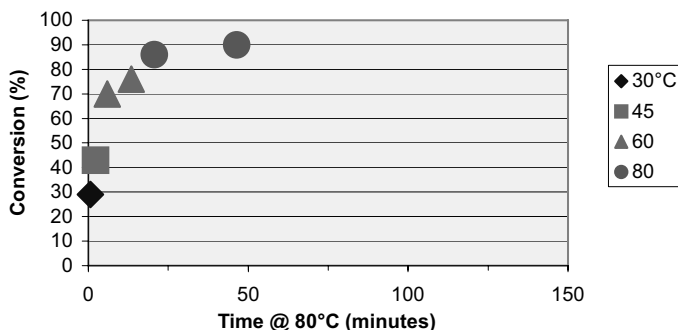


Figure 24.

Note that the highest conversion on this master curve is ~90%. To be truly representative values closer to 100% are needed. The difficulty in achieving this with isothermal cures is the interference of vitrification. Since vitrification does not occur in the actual process because the profile temperature quickly rises to above  $T_{g\infty} = 104^{\circ}\text{C}$ , it must also be avoided in the modeling. To accomplish this two data points were obtained from DSC cure profiles which simulated the process. The goal was to achieve one conversion just below 90% to overlap with the above master curve results and the other between 95 and 100%. To accomplish this DSC profiles were designed which would give equivalent isothermal times at 80°C ( $EIt_{80^{\circ}\text{C}}$ ) of ~35 and ~125 minutes, where  $EIt$  is computed by summing along the time-temperature profile as indicated in Eq. 3 below.



$$EIt_{80^{\circ}\text{C}} = \sum t_{80^{\circ}\text{C}} = \sum t_i [E(T-80) / R(T+273)(353)] \quad (3)$$

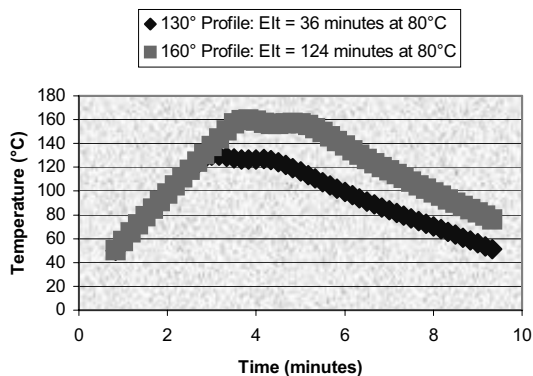


Figure 25.

Fig. 25 shows the DSC profiles together with their respective EIt computations. Samples were cured according to these profiles and their conversions determined from 10°C/min scans. These results were added to the master curve to give a Version 2 master curve, shown below.

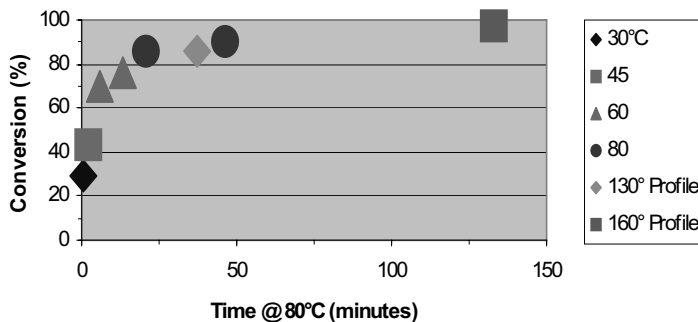


Figure 26.

In Step 3 data from the Version 2 master curve are analyzed to determine  $f(\alpha)$ . The data appear to have a general  $n$ th order shape. The cure is clearly not autocatalytic, missing the characteristic inflection. The general form of the  $n$ th order equation is

$$d\alpha/dt = k f(\alpha) = k (1-\alpha)^n \quad (4)$$

where  $k$  is the rate constant and  $n$  is the order of the reaction. The data were fit to 1<sup>st</sup> and 2<sup>nd</sup> order forms of the  $n$ th equation shown below

$$\text{1st order, } n=1: -\ln(1-\alpha) = kt \quad (5)$$

$$\text{2nd order, } n=2: 1/(1-\alpha) = 1 + kt \quad (6)$$

The data exhibited a very poor fit to the 1<sup>st</sup> order equation but an excellent fit to the second order equation, Eq. 6, with a high correlation coefficient as shown in Fig. 27. From the above 2<sup>nd</sup> order equation the slope, 0.235, is the rate constant at 80°C.

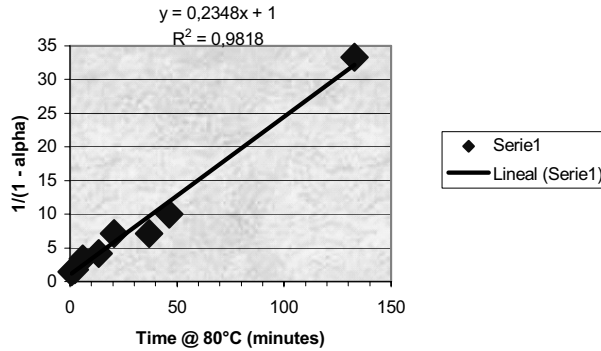


Figure 27.

Step 4 may now be addressed. With  $E$ ,  $f(\alpha)$  and  $k_{80^\circ\text{C}}$  known the pre-exponential factor can be computed from the Arrhenius equation, Eq. 1, as  $2.88\text{E-}10$ , providing a complete mathematical description of cure. From this kinetic equation the development of conversion along the profile shown initially was determined. The  $\text{EIt}_{80^\circ\text{C}}$  for the profile was computed to be 115 minutes from which a conversion of 96.5% may be estimated. The kinetic equation for cure also allows the computation of the master curve as shown in Fig. 28 below.

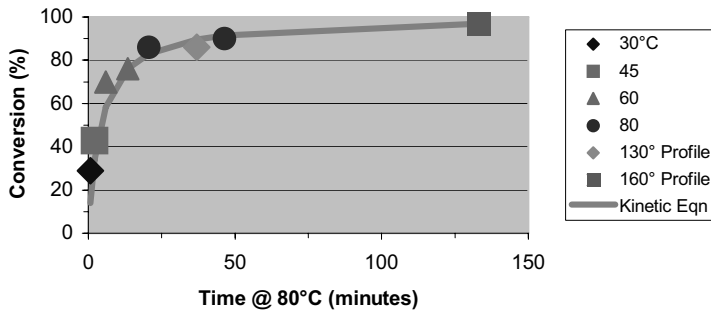


Figure 28.

## References

1. R. B. Prime, Chapter 6 "Thermosets" in Thermal Characterization of Polymeric Materials (E. A. Turi, ed.) Academic Press, San Diego (1997).
2. H. H. Winter, *Polym. Eng. Sci.* 27, 1698 (1987).
3. H. H. Winter, et al. in Techniques in Rheological Measurement (A. A. Collyer, ed.) Chapman and Hall, London (1997).
4. G. Wisanrakkit and J. K. Gillham, *J. Appl. Poly. Sci.* 42, 2453 (1991).
5. A. T. DiBenedetto, *J. Polym. Sci., Par B: Polym. Phys.* 25, 1949 (1987).
6. R. A. Venditti and J. K. Gillham, *J. Appl. Polym. Sci.* 64, 3 (1997).
7. B. Van Mele et al., *Thermochim. Acta* 266, 209 (1996).
8. H. E. Bair, D. J. Boyle, A. L. Young, and K. G. Steiner, *Soc. Plast. Eng. [Proc. Annu. Tech. Conf.]* 33, 262 (1987).
9. M. A. Best and R. B. Prime, *Proceed. SPIE Int. Soc. Opt. Eng.* 1774, 169 (1992).
10. R. B. Prime, unpublished data.
11. R. B. Prime, C. Michalski and C. M. Neag, *Proceed. 31<sup>st</sup> NATAS Conference*, Albuquerque, NM, (2003).